Nano Communication Networks 29 (2021) 100363

Contents lists available at ScienceDirect

Nano Communication Networks

journal homepage: www.elsevier.com/locate/nanocomnet

Beamforming optical antenna arrays for nano-bio sensing and actuation applications

Amit Sangwan *, Josep M. Jornet

Ultrabroadband Nanonetworking Laboratory, Department of Electrical and Computer Engineering, Northeastern University, Boston, MA, United States of America

ARTICLE INFO

Article history:
Received 28 January 2021
Accepted 17 May 2021
Available online 21 May 2021

Keywords:
Optical nano-antennas
Nano-antenna arrays
Nanonetworking
Nano-bio-sensing
Nano-bio-actuation

ABSTRACT

Light is found at the basis of bidirectional interfaces between digital systems and biological systems, including those in nano-bio-sensing and nano-bio-actuation applications. Despite the potentially very small size of optical transceivers and antennas, enabled by the very small wavelength of optical electromagnetic radiation, currently, existing systems commonly rely on macro-sized and intrusive equipment, including table-top microscopes and spectroscopy systems, and fiber optical technology as opposed to wireless setups. These place several bottlenecks between the possibilities and the capabilities of these emerging fields. In this paper, a unified theory is developed to design optical nano-antenna arrays, which are able to manipulate light similarly to how antenna arrays manipulate RF radiation. First, the applications of optical nano-antenna arrays in transmission, reception and reflection are described. Then, the fundamental factors affecting the design of individual optical antennas are described and modeled. The mutual coupling between optical nano-antenna is studied to guide the development of compact antenna arrays. Different beamforming strategies are proposed, and their performance is numerically investigated by means of finite element methods.

1. Introduction

Light plays a critical role in nature and it is found at the basis of numerous applications. Compared to other forms of electromagnetic radiation such as radiowaves and microwaves, light is characterized by very high frequency, very small wavelength, and high photon energy. Thanks to this high photon energy, light–matter interactions are possible. Also, because of the very small wavelength, nanoscale interactions are feasible. Harnessing these interactions we can enable communication with small devices at the nanoscale. One of the key application areas for such communications is in nano-bio sensing and nano-bio actuation. On the one hand, nano-bio sensing is the use of such interactions for detecting and monitoring biological processes at the molecular scale through engineered nanostructures such as nanoparticles or nano-engineered surfaces [1–4]. Nano-bio actuation, on the other hand, leverages these interactions to control the biological processes. Fields such as optogenetics and optogenomics leverage the use of light-based actuation systems to control the behavior and function of cells at genomic level [5].

Despite the small wavelength, current technologies used in these fields are not nanoscale and, in many occasions, not wireless, thus limiting the potential applications. For example, the majority of groups currently working on state of the art plasmonic nano-sensors use bulky equipment setups to read the data from sensors in ex-vivo measurements (e.g., in blood samples [1]). Also, the nano-actuation experiments that require the use of light to control biological processes at nanoscale use bulky optical setups [6]. In both cases, when it is required to confine light to a small region, optical fibers offer a practical solution. However, the use of fibers to inject light in body is extremely invasive and not adjustable or re-configurable once deployed.

In our vision, small wireless devices can be utilized for such precise nano-bio sensing and nano-bio actuation with a single cell or even sub-cellular resolution. Utilizing the same physics of radio frequency (RF), we can engineer optical nano-antennas and nano-antenna arrays (Fig. 1) to effectively and precisely illuminate the cells or specific regions of cells with unprecedented accuracy or, reciprocally, detect light in reception. Optical nano-antennas and nano-antenna arrays have been proposed earlier [7,8], but a unified approach to their design and, more importantly, dynamic control strategies of such arrays is missing.

In this paper, a unified theory is provided to design and develop optical antenna arrays, starting from the design of a single antenna element and the relative placement of separate elements in the presence of mutual coupling. We also describe

* Corresponding author.
E-mail addresses: amit@northeastern.edu (A. Sangwan), jmjornet@northeastern.edu (J.M. Jornet).

https://doi.org/10.1016/j.nancom.2021.100363
1878-7789/

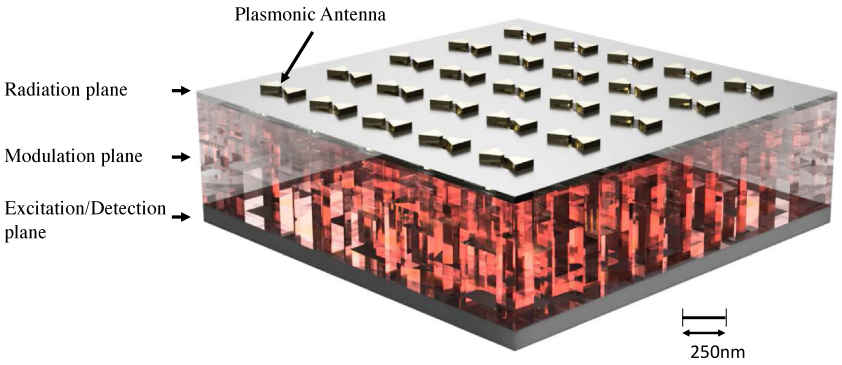

Fig. 1. Conceptual representation of how an integrated beamforming optical nano-antenna array device might look like.

different beamforming strategies that could be used with optical nano-antenna arrays. In addition, we numerically investigate the performance of such techniques along with the complexity of implementing them.

The rest of the paper is organized as follows: In Section 2, we present the related work and background information to the topic. In Section 3, we present the application areas for the work. In Section 4, we present the fundamentals for designing the nano-antenna array at optical frequencies and the beamforming architecture. In Section 5, we present the beamforming and control strategies for the optical nano-antenna array. In Section 6, we present numerical analysis and its results. In Section 7, we provide some conclusions from the results.

2. Related works

There have been several recent advancements in optical technology that pave the way to enable more advanced micro/nano applications of light. We summarize them in this section.

2.1. Optical antennas

Optical antennas are nano-structures that efficiently convert optical currents into light radiation and vice versa. The term optical current is used to describe either electrical currents at optical frequencies (i.e., in an electrically driven optical antenna) or a photonic current (i.e., in a laser-pumped optical antenna or in a photonic integrated circuit followed by an optical antenna).

As we describe in Section 4.1, the geometric design of optical antennas is mostly governed by the same principles as of the design of antennas at lower frequencies. However, the much smaller wavelength of optical signals leads to a much more challenging fabrication process. For the time being, different types of optical antennas have been demonstrated, including dipole antennas [9–11], bow-tie antennas [12–14], Yagi–Uda antennas [15,16], slot-antenna [17–20], patch antenna [21,22] and cross-antenna [23]. The fabrication of the majority of these antennas involves the use of Focused Ion-Beam (FIB) milling or Electron Beam Lithography (EBL) and some even newer and more precise nano-fabrication [24–26].

In these previous works, the optical antennas were driven through an external light source, which is less complex than attempting to embed an optical signal source with the antenna. Nevertheless, some recent works have reported success in electrically excited optical antennas [27,28]. These antennas involve using the photon-tunneling effect at the source cavity to generate the signals and antenna structure as the filter and efficient radiator.

2.2. Optical antenna arrays and optical metasurfaces

While this is a less mature area of research, optical antenna arrays are gaining the interest of the research community for their unique ability to control the output wavefront and, thus, providing the ability to do beam shaping at optical frequencies [8]. As in an antenna array at lower frequencies, the fundamental idea is to enhance the radiated signal in specific directions by manipulating the phase or time delay in which the signal at different elements of the array is radiated (or reciprocally processed). For the time being, optical antenna arrays are limited by static phase shifting elements, i.e., the phase control at each element is passive and, hence, dynamic beam steering is not supported.

From the design perspective, metasurfaces are fundamentally similar to an optical antenna array for its function and design [29]. Metasurfaces take advantage of the precisely designed structures that allow phase control at sub wavelength resolution and therefore enabling the control of resultant wavefront. This control in a planar structure has allowed the use of these technologies for applications that earlier required optical elements. Along with that, the same technology can also be used to design metamaterial filters [30–32] and polarizers [33,34] to selectively target a particular frequency from a wide-band source. The majority of applications of such optical antenna arrays has played a key role for in flat optics [35]. However, some groups have also tried to actively shift the phase [7] but the low power and low coupling efficiency has limited the application of such designs.

In this paper, we present a scalable design with a unified framework for beamforming antenna arrays that allows high coupling power and the dynamic control of the beam from optical arrays.

3. Applications of optical nano-antennas and nano-antenna arrays in nano-bio-sensing/actuation

Optical nano-antenna arrays, similar to their RF counterparts, follow the principle of reciprocity. As a result, antenna arrays can be used in transmission, i.e., to convert electrical signals to EM radiation, as well as in reception, i.e., to couple EM radiation and convert it to electrical signals. In addition, as a combination of the two functionalities, these can also be used in reflection (reception plus transmission), and all of these while performing beamforming. Such unique control of optical waves at the nanoscale enables a variety of novel applications. In this section, we describe some of the most unique applications of optical nano-antenna arrays for nano-bio-sensing and -actuation, classified by where the array plays a key role, namely, at the transmitter (i.e., as an actuator), at the reflector (i.e., as a sensor) or at the receiver (i.e., as a detector).

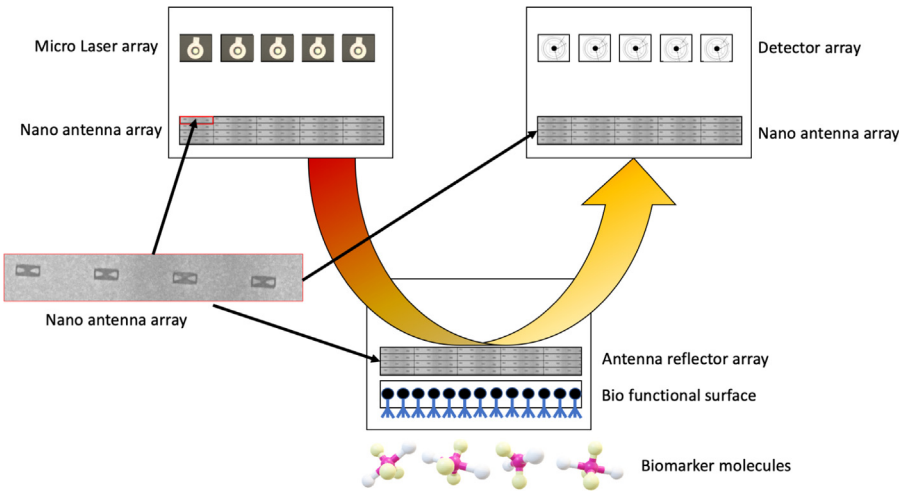

Fig. 2. An overview of applications of nano-antenna arrays in nano-sensing systems.

3.1. Applications in transmission: optogenetics and optogenomics

An optical antenna array can function as an effective radiating structure and, when coupled with active phase control, can allow dynamic beamforming. This dynamic beamforming can enable precise nano-scale selective focus of light to maximize the signal to noise ratio at target locations.

One of the key applications of such precise beam control in the transmission is in the field of optogenetics and optogenomics. Recently, major breakthroughs in the field of biophotonics and genomics are enabling the control of biological processes through light [5]. By incorporating light-actuated and light-emitting proteins into cells, key biological processes at the single-cell and even sub-cellular level can be controlled in real time [36,37]. For the time being, scientists have mostly been combining optics and genetics into *optogenetics*, with the primary goal of employing light to control cell–cell interactions. Such techniques are focused on manipulating the cell activities in multi-neuronal networks and, thus, are also referred to as optoneuronal platforms.

Our recent work [5] and ongoing investigations focus on creating a new subfield of research that we refer to as *optogenomics* or light-based control of the genome's function. While the applications of this new paradigm are uncountable, our initial goal is to demonstrate the feasibility of controlling cellular development, including information processing and learning. Cell development and fate may be influenced by targeting individual genes and even more effectively by globally controlling the 3D genome architecture [38]. By targeting the recently described pan-ontogenic Integrative Nuclear FGFR1 Signaling (INFS) in developing neuronal cells, we can influence the genome structure and function and, thereby, develop neuronal networks and their ability to process and learn information [5,38].

While conventional optical sources can be utilized to trigger system-wide responses, being able to control individual cells will open the door to the study of the cell functions within complex tissues and organs. For example, we can utilize beamforming nano-antenna arrays to independently program (optogenomics) and/or activate (optogenetics) cells, enabling interesting studies of, for example, signal and change propagation in neuronal networks, as well as single-cell therapies. Moreover, in a more ambitious vision, multiple nano-devices (or nano-machines) acting in a coordinated fashion can develop complex cell networks(neurons or muscle fiber tissues) from stem cells.

3.2. Applications in reflection: plasmonics-enabled nano-bio-sensing

One of the very first applications of optical nano-antennas was precisely in the field of nanosensing. Nanotechnology has enabled the development of novel nanosensors that are more precise and much smaller than the traditional sensors. Plasmonic sensors [39], among all other nanosensing technologies, have gained popularity in the last decade for compact sensing systems. A plasmonic sensor works on the principle of surface plasmon resonance (SPR) effect. The SPR effect is a result of the interaction of light and matter at the nano-scale. The design of an SPR-effect-based sensor consists of a metallic or conductive resonating structure with a bio-functionalized surface that selectively combines to desired bio-marker molecules. This combination changes the resonating response of the structure, which can be then analyzed using an optical system to determine the sensing results. To interact and read information from these sensors at this nano-scale, we must use small-wavelength (optical range) sources and very sensitive detector systems. One of the most common resonant structures are nanoparticles, which are many times referred to as nano-antennas in the nanosensing literature. Recently, researchers have demonstrated the feasibility of these sensors for in-vivo nanosensing systems and demonstrated their ability to accurately detect disease biomarkers for cancer [40] and other such diseases.

In addition to enhancing the capabilities while reducing the size of the excitation and measurement system of nanosensors, optical antenna arrays can also be designed to enhance the sensor itself.

In particular, the advancement of antenna array technology has allowed us to create intelligent reflector arrays, also known as smart or intelligent reflecting surfaces, at different frequencies across the spectrum [41–44]. In our vision, a similar concept can be leveraged in nanosensing applications. As shown in Fig. 2, an optical reflect-array can be designed to reflect the incident power at the desired angle and with the desired beam pattern. For detection, the target biomarkers' presence might manipulate the strength of the reflection or even the direction of the same, hence opening the door for different detection mechanisms in nanobiosensing.

3.3. Applications in reception: super-resolution microscopy

As with the transmitter, an immediate application of optical antenna arrays is to enhance the detected power at the receiver. Among others, microscopy was limited by the diffraction limit of

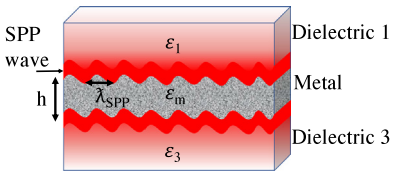

Fig. 3. SPP waves at metal–dielectric-metal interfaces for thin metal.

optical lens setups until it was demonstrated that using a metal nano-particle at the end of a fiber tip could significantly enhance the near field coupling to fiber and overcome the diffraction limit [45]. Thus, the first nano-antenna was validated practically for microscopy. Since then, there has been active research on the topic [46,47], and different nano-structure on fiber tip has been experimented with to enhance the coupling to fiber to enable super-resolution imaging. These nano-structures use the same principles as optical nano-antennas and benefit by using Surface Plasmon Polariton (SPP) waves, which allow them to be much smaller than the free-space wavelength, thus to overcome the diffraction limit. Using optical nano-antenna array in super-resolution microscopy can result in the more precise and fast scanning of samples. Beamforming from the optical nano-antenna array can provide even more selective non-mechanical scanning options and sub-diffraction limit focus.

4. Design of optical nano-antenna arrays

In this section, we provide an overview of the physics involved in the function of an optical nano-antenna and the equations governing its geometric design. We then extend this single-element analysis to the design of an array, with an emphasis on the mutual coupling between elements.

4.1. Optical nano-antenna

The design process of a nano-antenna is different from that of a traditional antenna. Traditional antennas are built with metals or, effectively, perfect electric conducting (PEC) materials in which electromagnetic waves cannot penetrate. As a result, they resonate at the electromagnetic wavelength defined by the surrounding air or effective medium permittivity. Instead, as a result of the lack of PEC materials at optical frequencies, the resonant frequency of an optical nano-antenna also depends on the complex permittivity of its building material. Indeed, at optical frequencies, the electromagnetic waves can propagate within the so-called penetration depth of the material. We refer to these surface waves at metal–dielectric interface as SPP waves. Therefore, designing an optical nano-antenna requires the knowledge of the material properties at optical frequencies and the equations describing both SPP waves and free-space propagating electromagnetic waves.

The Drude and Lorentz model provides an accurate description of the complex-valued conductivity and permittivity of metals at optical frequencies [48,49]. In particular, the frequency-dependent permittivity ε_m of a metallic sheet is given by [50]:

$$\varepsilon_m = \left[\varepsilon_m(\infty) - \frac{\omega_p^2\tau_d^2}{1+\omega^2\tau_d^2} + j\frac{\omega_p^2\tau_d}{\omega(1+\omega^2\tau_d^2)}\right], \tag{1}$$

where ε_m is the permittivity of the metal, ω_p is the plasmonic wave frequency of the material, τ_d is the electron relaxation time, $\epsilon_m(\infty)$ is the permittivity of metal when the metal sheet is infinite in width and $\omega = 2\pi f$ is the angular frequency.

Starting from the frequency dependent complex permittivity, the propagation wave constant of SPP waves can be obtained by solving their dispersion equation for the particular structure under study. More specifically, for a system composed of dielectric-metal–dielectric interface (Fig. 3), the complex-valued SPP wave vector, k_{spp}, can be obtained by solving [51]

$$k_{spp} = (\varepsilon_1\varepsilon_3 S_3^2 + \varepsilon_m^2 S_2 S_3)\tanh(S_2 h) + \varepsilon_m S_2(\varepsilon_3 S_1 + \varepsilon_1 S_3) \tag{2}$$

$$S_1 = \sqrt{\beta^2 - \varepsilon_1 k_0^2}, \tag{3}$$

$$S_2 = \sqrt{\beta^2 - \varepsilon_m k_0^2}, \tag{4}$$

$$S_3 = \sqrt{\beta^2 - \varepsilon_3 k_0^2}, \tag{5}$$

where $k_0 = \omega/c$ is the free space vector, β is the complex propagation constant parallel to the surface, ε_1 and ε_3 are the permittivity of the layers surrounding the metal sheet, and ε_m is the permittivity of the metal as described in (1) . Therefore, the SPP wave properties will change not only according to the antenna building materials, but also with the surrounding media.

Finally, for this structure to become resonant, its length should be finite and equal to half of the plasmonic wavelength [48,50,52]. The SPP wavelength is expected to be smaller than that of the free-space wavelength, which ultimately leads to smaller antennas.

For some designs, the response of the antenna can be obtained analytically and in closed form. For example, the radiated fields by a plasmonic nano-dipole antenna are provided in [53,54]. However, this is not the case for more general designs, including patch, bow-tie and other non-traditional antenna geometries. Because of that, we rely of Finite Element Methods (FEM) to accurately predict the performance of the nano-antenna designs.

4.2. Antenna array

There are several considerations to take into account when moving from the design of individual antennas to their integration into dense antenna arrays. For an antenna array to exhibit beamforming gain, the total antenna footprint should span at least half of the free-space wavelength or $\lambda_0/2$. At the same time, to prevent the presence of grating lobes, individual antennas cannot be more than $\lambda_0/2$ apart. Given the fact that $\lambda_{spp} \leq \lambda_0$, this is not a challenge for optical nano-antennas. However, the placement of the antennas in close proximity can lead to mutual coupling effects, which ultimately can hamper the performance of the array. Therefore, to design optical nano-antenna arrays, we need to model and predict the mutual coupling between adjacent structures (Fig. 4) and the effect of the distance D_x and D_y on the resonating frequency of the structure.

Mutual coupling between elements of the array leads to a change in the element input impedance, which effectively leads to a change in the resonant frequency of the antenna or, conversely, in the power at the original design frequency. Traditionally, antenna arrays are designed to avoid mutual coupling. Alternatively, arrays could be designed to leverage mutual coupling or, in other words, make a coupling-aware design. Whether to avoid it or to take into account in the design, there is a need to predict the mutual coupling up front.

There are different approaches to predict the mutual coupling. For example, in [55], coupled mode theory is utilized to estimate the mutual coupling between neighboring antennas. A mathematical analysis is provided along with numerical simulations of a two element array, which exhibit how the strength of mutual coupling changes with respect to the separation distance.

Here, instead we tailor the methodology used for non-plasmonic antennas from [56] to the case of optical nano-antennas. Following this general approach, we define the mutual impedance

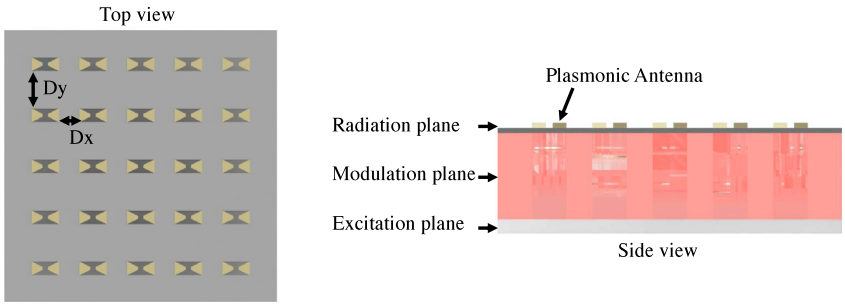

Fig. 4. Mutual coupling: effect of a neighboring resonator distance on the resonating frequency.

between a transmitting element and its immediate neighboring antenna elements in the array as:

$$Z_{12} = \frac{V_1}{I_{2|V_2=0}}, \tag{6}$$

where Z_{12} is the impedance of Antenna 1 when Antenna 2 is in proximity, V_1 is the excitation voltage of Antenna 1 and $I_{2|V2=0}$ is the current in Antenna 2 when the excitation voltage in Antenna 2 is zero. To fully analyze the effect of the neighboring element, we need to excite the Antenna 1 while changing the position of Antenna 2 around it, then measure the effect of the position of Antenna 2 on the impedance of Antenna 1. Because of the limited availability and feasibility of performing such experiment for optical antennas, we need to perform a FEM analysis to predict the inter element distance.

As we will discuss in Section 6, the much smaller size of the plasmonic elements also leads to a reduced coupling between them. Particularly, compared to microwave antennas made from PEC material, in which the mutual coupling is determined by the free-space wavelength, in plasmonic antennas, the mutual coupling is determined by the plasmonic wavelength. As a result, the antenna elements can be placed even closer, thus, allowing for a denser array.

5. Beamforming and control architecture

Antenna arrays by themselves are able to provide high directivity gain, but unless they support dynamic control, there is no major advantage over using an optical dielectric lens or a metamaterial flat lens [35]. To dynamically adjust the pattern of the radiated beam, precise phase control at each element is needed. The process of maximizing the radiated power in a given direction (or, reversely, minimized in other directions) is known as beamforming. In this section, we present different architectures to enable beamforming with optical antenna arrays, which leverage the properties of plasmonic structures.

5.1. Principle of beamforming

The process of beamforming relies on the phenomenon of constructive and destructive interference of the radiated electromagnetic fields by each element. The direction in which signals constructively or destructively overlap can be controlled by engineering the phase or, reciprocally, the delay of the signal at each individual antenna element. For a light wave to travel in a particular direction, the phase on the wavefront should be same. As it can be seen in Fig. 5, for a wavefront in direction θ_0 the signal has to travel an additional distance of $dsin(\theta_0)$. Generalizing it to a n-dimensional linear array, we can write the expression for the phase difference β between elements for a linear 1-dimensional array to achieve beamforming in the desired angle θ_0 [57]:

$$\beta(\theta_0) = \frac{2\pi d \sin\theta_0}{\lambda_0}, \tag{7}$$

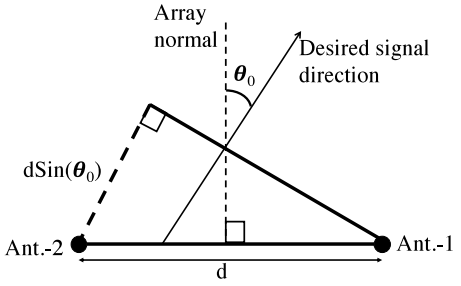

Fig. 5. Beamforming from 2 antenna elements at an angle θ_0 from normal.

where d is the inter-element distance.

Similarly, in a two-dimensional array, we can manipulate the direction of the beam to be steered left/right and up/down. For a n by n uniformly spaced rectangular array to create a main beam at $\theta = \theta_o$ and $\psi = \psi_o$, the progressive phase difference between elements in x and y direction is given by [57]::

$$\beta_x(\theta_0, \phi_0) = \frac{2\pi d_x \sin\theta_o \cos\phi_o}{\lambda_0}, \tag{8}$$

$$\beta_y(\theta_0, \phi_0) = \frac{2\pi d_y \sin\theta_o \cos\phi_o}{\lambda_0}, \tag{9}$$

where θ refers to the elevation angle and ϕ refers to azimuth angle, (θ_o, ϕ_o) is beam pointing direction, d_x and d_y is the inter-element spacing along x and y axis respectively.

5.2. Phase control strategies

To implement beamforming in the proposed optical antenna array, we require the ability to control the phase in modulation plane. In the following section, we present strategies for the phase control of optical signals.

5.2.1. Delay line phase prediction

The design of a delay line involves leveraging the fact that light travels at different speeds in different materials and this speed is proportional to the refractive index of the material. Taking advantage of this property, if we control a collimated beam of light (parallel beams with same phase) to travel the same path length in two different mediums, then we can achieve predictable relative phase shift. The delay needed to steer a beam to a desired angle θ_o in a uniform linear array with inter-element spacing d is given by:

$$\Delta t = \frac{d(\sin\theta_o)}{v_o}, \tag{10}$$

where v_0 is the speed of light in the given medium. This will produce the same phase difference given by (7).

Using the relation between speed of the electromagnetic wave and the material refractive index, we can design a delay line to

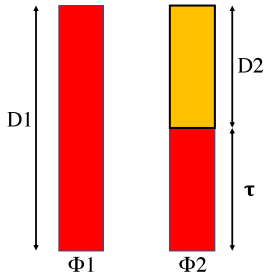

Fig. 6. Phase delay due to the delay line in same medium.

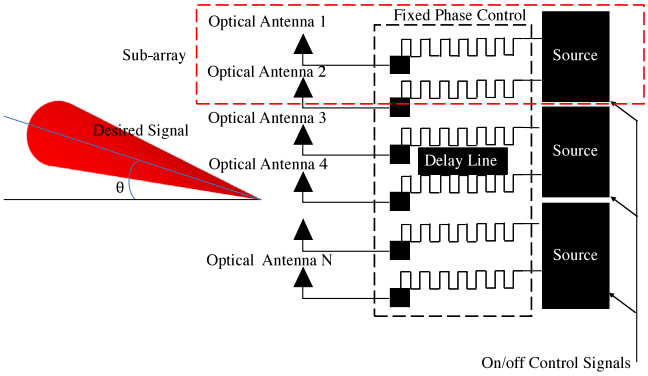

Fig. 7. Architecture of the proposed array for excitation plane control.

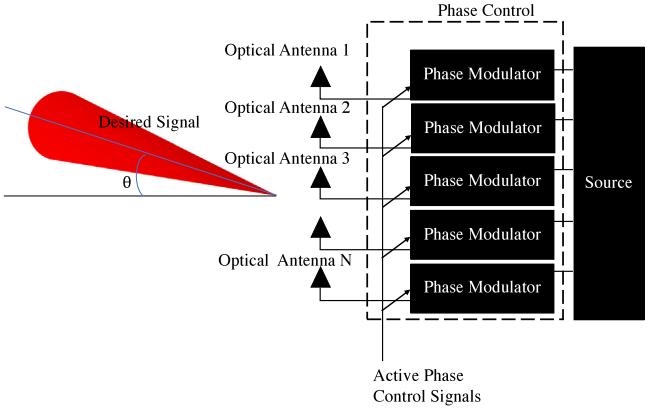

Fig. 8. Architecture of the proposed array for modulation plane control.

achieve a specific phase shift of $\Delta\phi$. The following equation gives the relation between the thickness $D2$ of a new material with refractive index n_2, needed to be placed to replace a medium of refractive index n_1 to achieve the desired phase shift $\Delta\phi$ at the end.

$$D2 = \frac{\Delta\phi}{2\pi}\frac{\lambda_{D2}\lambda_{D1}}{\lambda_{D1} - \lambda_{D2}} \tag{11}$$

$$\tau = D1 - D2 \tag{12}$$

where $\Delta\phi = \phi_2 - \phi_1$, ϕ_2 is the phase shift at the end of delay line 2 and ϕ_1 is the absolute phase shift at the end of delay line 1, also shown in Fig. 6. The effective wavelengths in medium 1 and 2 are $\lambda_{D1} = \frac{\lambda_{fs}}{n_1}$ and $\lambda_{D2} = \frac{\lambda_{fs}}{n_2}$, respectively, where λ_{fs} denotes free space wavelength.

The required width ($D2$) depends on difference in values of λ_{D1} and λ_{D2}, for the 1550 nm wavelength and a phase shift of $\Delta\phi$ of $\pi/4$ degrees using glass and PMMA it is generally in the few hundred-nanometer range. Alongside this, for a continuous monochromatic light signal, the length of these delay lines does not necessarily require to be constructed with nanometer-scale precision. However, it can be of length $(D2_{\Delta}\phi_2 + D1_{\Delta}\phi_{2\pi})$ producing the same $\Delta\phi$ at the end between the D1 and D2 lines. Another challenge is to achieve precise control at the scale of a few femtoseconds time resolution. Nonetheless, this is not a necessary condition, as such femtosecond-long delay is relative to the signal fed to adjacent elements and is not absolute control resolution.

5.2.2. Other mechanisms of phase shifting at optical frequencies

Achieving the phase control at optical frequencies on a chip is a challenging task. Recent advances in nanophotonics have demonstrated the feasibility of developing electro-optic nano-scale phase shifters [58] or modulators [59–61]. However, as these advances have made phase shifting at the optical bands possible, the hurdle is that they only work for a very narrow band of frequencies. Along with that, the designs should meet the constraints to be compact and stackable in a 2D antenna array arrangement. Most of the current advanced designs are in the planar XY plane. They do not offer the possibility of being fabricated along the Z-axis. Thus, it motivates us to use delay lines for the wideband response they offer and the fabrication facility they offer over other designs.

5.3. Beamforming architecture

We can leverage the work done in the RF domain to design an optical beamforming system. For the proposed compact design shown in the previous section, we can use two main architecture strategies. The first approach is to control the excitation plane (i.e., the source) in an on/off fashion. Thus, only enabling the antenna elements that are responsible for the desired angle. If we can have phase control at the signal source itself, such as the one demonstrated by Laferriere et al. [62] in a compact configuration, it would be achievable. Meanwhile, this approach is also consistent with using a delay line based phase shifter. The second approach is to perform dynamic phase and amplitude control in the modulation plane for each antenna element to enable beamforming. This approach is better suited when the dynamic phase shifter designs can meet the specification of Z-axis fabrication. On the optimistic side, if we achieve dynamic beamforming, we can leverage a hybrid of the first and the second approaches to implement dynamic beamforming to optimize power efficiency. This improved power efficiency can be achieved by selectively turning a few elements on/off, making it more suitable for the nano/micro battery-operated applications. Further details on these architectures are as follows:

5.3.1. Slotted beamforming architecture: control in the excitation plane

The best control would be to enable the source to emit precise signals with accurate phase information and then feed those signals to the individual antenna elements. Nevertheless, current state of art optical sources provide compactness [63], but not such precision. Hence, we target the control of the signals using delay lines and feed these controlled relative phase signals to the sub-array antenna elements. To achieve multiple beam-angles or to some extent beam-steering, we use a large array of these sub-arrays. These sub-arrays have their unique sources. By independently controlling sources on/off, we obtain the target direction of the resultant beam.

The proposed architecture is presented in Fig. 7. The relative inter-element phase shift required for a 2D array to target a beam angle at elevation angle θ and azimuth angle ϕ can be calculated using (8) and (9). The delay lines can be designed using (11) and

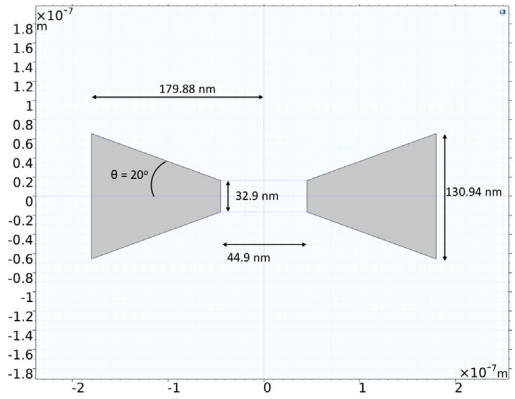

(a) Geometry of the bow-tie optical nano-antenna.

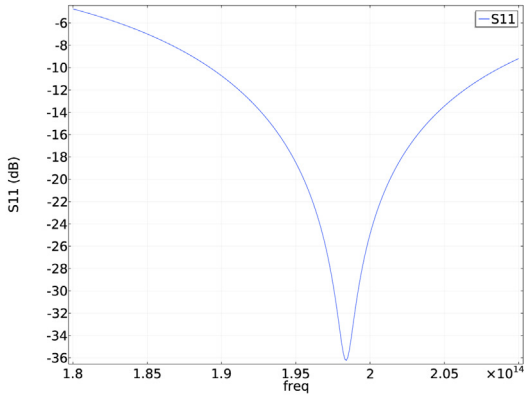

(b) S11 parameter

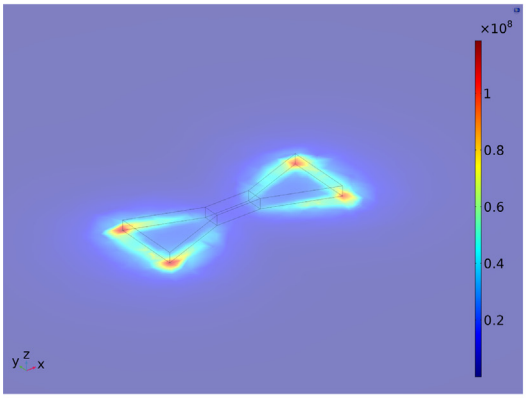

(c) Electric field distribution on the nano-antenna

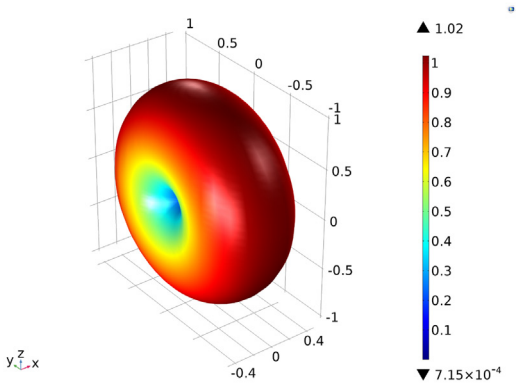

(d) Electric field distribution on the nano-antenna

Fig. 9. Numerical analysis of performance of the designed antenna.

(12) for a precise phase shift $\Delta\phi$. However, the shortcoming of using sub-arrays with fixed delay lines is that a large array of sub-arrays is needed for the flexibility to target desired angles. While, this added volume makes this approach bulky, considering the small size of the optical antenna elements, the overall size is still small and within millimeter constraint.

At this point, it is relevant to consider and discuss the advances in the field of metamaterials. Metamaterials has allowed for the ability to create flat lenses that can be directional. While usually flat nature provides them an advantage when compared to delay lines, existing metamaterial lenses are very narrow-band compared to delay lines, i.e., their response drastically changes with the operation wavelength/frequency. Nevertheless, for applications involving sensing, a broadband response is often preferred. Enabling the antenna element level controls also allow us to apply the knowledge, progress, and breakthroughs made in RF beamforming to optical wireless systems.

5.3.2. Adaptive beamforming architecture: control in the modulation plane

The beamforming architecture that can leverage the control of modulation plane (between the excitation plane and the radiation plane, Fig. 4) is presented in Fig. 8. Control in the modulation plane refers to dynamic phase control of signals fed to each antenna element. This precise control at each antenna element allows us to control the resultant beam angle adaptively. The phase required at each element is dependent on the direction chosen for the beam, i.e., θ_0 angle of elevation and ϕ_0 azimuthal angle. The relative inter-element phase shift required for a 2D array to target a beam angle at elevation angle θ and azimuth angle ϕ can be calculated using (8) and (9). Another advantage of using this architecture is that it can leverage a single source for all the nano-antenna elements. Hence, eliminating the need for a source of the scale of the nano-antenna element.

Nevertheless, another opportunity from using phase control is modulating the signal to carry data bits. We can also engineer the resultant beam to selectively target multiple angles. This architecture can leverage the vast literature existing for RF antenna arrays, which provides us multiple signal processing algorithms to leverage this to its full capacity. Thus, allowing a robust and compact transceiver set up in a layered form factor.

5.3.3. Hybrid architecture: joint control of excitation and modulation planes

As discussed in the previous section, control in the excitation plane and the modulation plane have their independent advantages. Excitation plane controls allow for a simpler architecture, while modulation plane control offers the freedom in adaptability. Using this architecture, we can perform a hybrid approach that can leverage both architectures' best. The possibility of controlling the excitation plane and modulation plane together offers the ability to address the device's power efficiency aspect. Most compact applications such as wearable and mobile devices have limited power available from a battery. This limited budget becomes a significant problem and, therefore, should be addressed. Ability to have a very dense array and control over the fact that we can turn few elements on/off can change the power budget required for the operation and communication. This dynamic change allows us to consume less power for the close-range communication needs allowing less power per bit

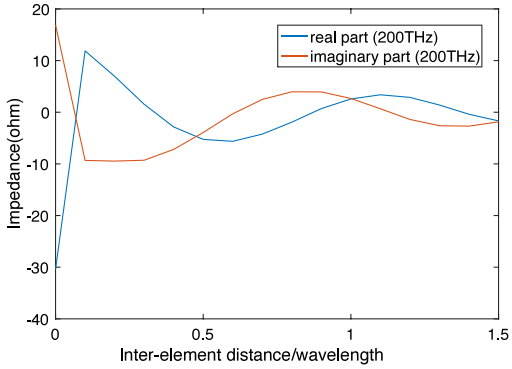

(a) Mutual coupling affecting impedance of antenna element in the array as function of x-axis separation distance.

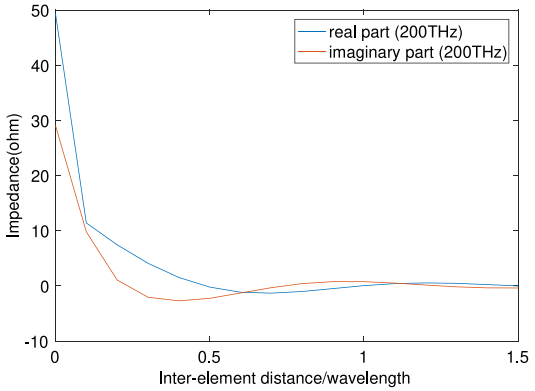

(b) Mutual coupling affecting impedance of antenna element in the array as function of y-axis separation distance.

Fig. 10. Effect of inter-element spacing of antenna array on antenna impedance.

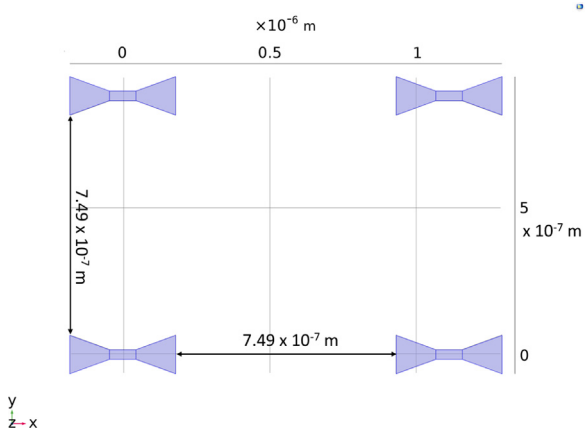

Fig. 11. Designed bow-tie antenna array dimensions. Antenna element labeled in clockwise order from left bottom: Antenna 11, Antenna12, Antenna 22 and Antenna 21.

transmitted. Simultaneously, we can turn on all the elements that allow us the long-range needed for accurate detection for long-range applications.

Another added benefit from this architecture is its resiliency to faults. The hybrid architecture can tolerate faults and still function. The faulty elements can be disabled. Thus, we can leverage the improved efficiency and minimize the interference caused by the faulty antenna elements.

6. Numerical analysis results

In this section, we use FEM modeling with COMSOL Multiphysics to numerically design, model and analyze the performance of optical nano-antenna arrays.

6.1. Antenna design

We select a bowtie antenna as the building block of optical antenna arrays due to its broadband nature. Hence, we can support a variety of wavelengths for the transmission around the given designed frequency. Using (1), we calculate the permittivity for gold as a function of frequency. Gold has plasma frequency ω_p = 13.35 PHz and electron relaxation time $\tau_d = 10$ fs.

Table 1
Geometrical parameters used to design an optical bow-tie antenna.

Parameter	Value
Bow length	179.88 nm
Bow width	130.94 nm
Bow angle	20°
Port length	44.9 nm
Port width	32.9 nm
Antenna thickness	20 nm

In our analysis, we conduct extensive numerical simulations with COMSOL Multiphysics to optimize the optical bow-tie antenna design. The final design parameters are summarized in Table 1 and illustrated in Fig. 9(a).

For a perfect electric conductor, the ideal length of a half-wave dipole antenna is $\lambda/2$. For our design wavelength of 1550 nm, free space $\lambda_0/2$ is 750 nm. However, because plasmonic waves are shorter than free space waves, the designed antenna length is 360 nm for our gold-based antenna structure.

The simulated antenna performance is presented in Fig. 9. The radiation pattern is similar to that of a dipole antenna, i.e., ring-shaped. The S11 parameter shown in Fig. 9(b) describes the reflected power losses shows that this designed antenna can work efficiently at the range of 1.9 THz - 2.1 THz (with less than -10 dB loss).

6.2. Antenna array design

The dimensions of the array antenna elements are as per the design in Section 4.1. The inter-element spacing for the antenna array should be as such that it should not affect the entire array's resonant frequency. Hence, we performed a parametric sweep to calculate the ideal inter-element spacing. During this sweep, we fixed one antenna and we observed the neighboring antenna's effect on the antenna's impedance while changing the inter-element distance along the X and Y-axis. Fig. 10 presents the results demonstrating the effect of inter-element spacing on the antenna impedance. Thus, we select the spacing of 749 nm, which minimizes the mutual coupling between the antenna array elements. Reducing inter-element spacing seems lucrative, but reducing it beyond a limit will result in the coupling effect causing the losses due to a resonating frequency shift. While increasing it too much would result in side lobes' generation resulting in a less focused beam. The geometry of the array is as per Fig. 11.

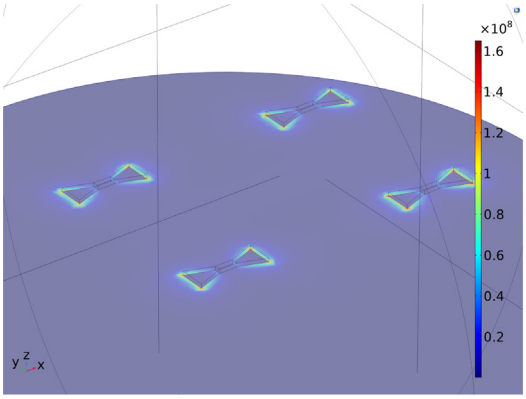

(a) E-field distribution of the designed bow-tie antenna array.

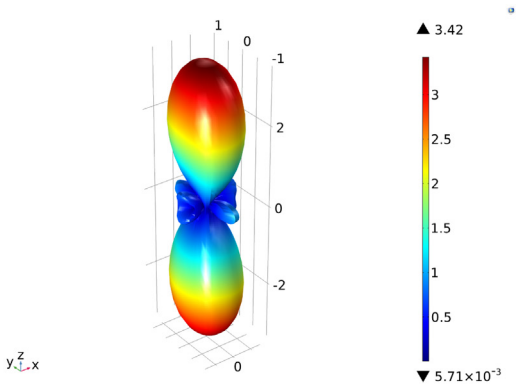

(b) Far field analysis of array with no phase difference between elements.

Fig. 12. Performance of designed bow-tie antenna array.

6.3. Performance

To calculate the array factor and demonstrate beamforming, we conceived an antenna array of 4 elements. The E-field distribution on the antenna array elements is presented in Fig. 12(a). For the simplification of the simulation model, each element has its unique independently controlled source, following the architecture shown in Fig. 8. To calculate the beam pattern of the array, we are using the far-field model. Fig. 12(b) shows the array factor of design with no shift between antenna elements. The results of Fig. 12(b) exhibit that the design is of a broadside array.

6.4. Delay-line based phase control

Simulating a phase control at the port of excitation is preferred in favor of the model's computational complexity minimization. However, to realize a beamforming architecture, the phase shift mechanism should also be validated. In previous section, we propose the design of delay lines as per (11) and (12) for a precise phase shift $\Delta\phi$. To validate this design approach, we modeled two lines. In the first line, we used the same material, and in the second line, we designed the length of the line to result in the phase shift of $\Delta\phi = pi/4$. We simulated the model with Electromagnetic physics and wave equation for transient analysis in COMSOL. The results shown in Fig. 13 confirm the phase delay and, thus, confirm the functioning of the delay line. These results provide promising results for controlling the relative phase at individual elements of the antennas array, thus catering to the fundamental need for beamforming.

6.5. Beamforming performance

To evaluate beamforming performance of the designed array, we used far-field analysis and phase control at the individual antenna ports. The antenna array uses the designed optical antenna elements, as in Section 4.1. This approach allows for numerical analysis with reduced computational complexity. Fig. 14 presents the results of beamforming performance from the array for the configurations presented in Table 2. We observe that the antenna array's main beam can be steered in the desired direction with the proper control of the relative phase between antenna elements. These results demonstrate directional gain and the feasibility of dynamic control for the optical antenna array.

In addition to evaluating the beamforming performance we also numerically compared slotted and adaptive beamforming

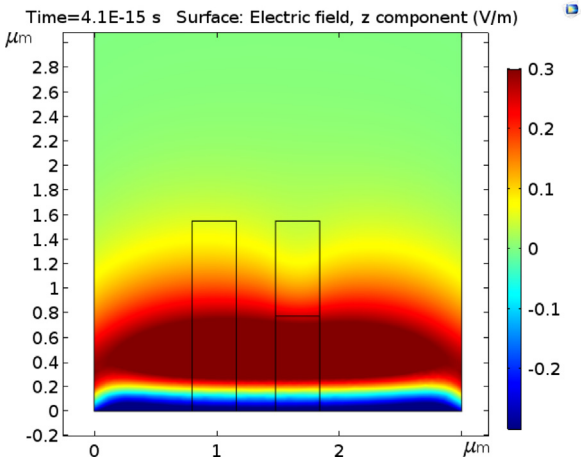

Fig. 13. Numerical analysis of phase delay due to the delay line.

architectures for the antenna arrays. With on/off control of the slotted architecture we can see that the beampattern is much wider for the same footprint of the overall array. While with adaptive all the elements are turned on and with adaptive phase change we can have a merit of narrower main beam width and higher directivity compared to same footprint size (see Fig. 15).

7. Conclusions

Light plays a key role as an interface with biological systems. By developing compact tools to manipulate light at the nano- and micro-scopic level, we can interact with the building blocks of living systems. In this paper, we have developed a unified framework to design optical nano-antenna arrays that can be used in transmission, reception and reflection for nano-bio-sensing and nano-bio-actuation purposes. While still several fabrication-related challenges need to be addressed, including the integration of antenna arrays with a large number of elements with the given tight tolerances or the 3D-integration of the excitation, modulation and radiation plane, the underlying theory and, thus, possibilities are defined.

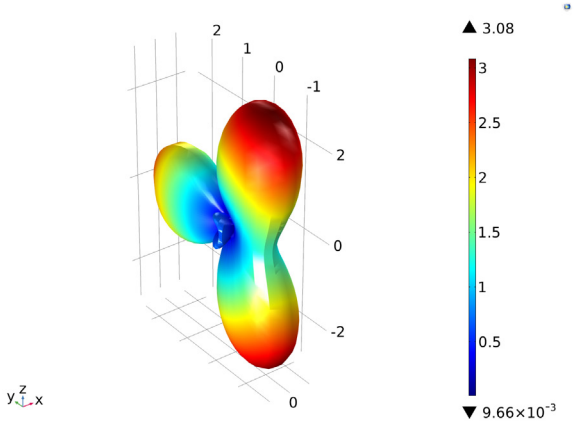

(a) Case 2:Beam steered towards -y direction

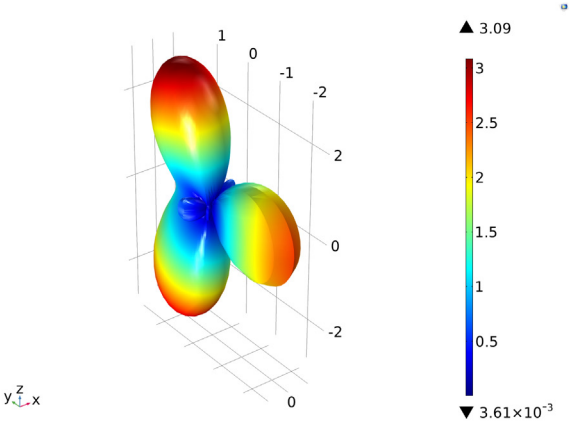

(b) Case 3:Beam steered towards +y direction

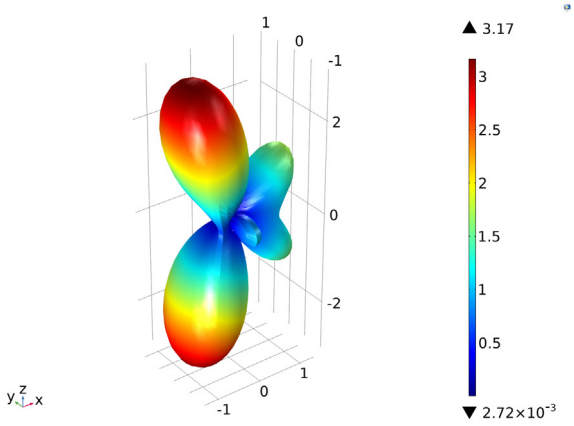

(c) Case 4:Beam steered towards -x direction

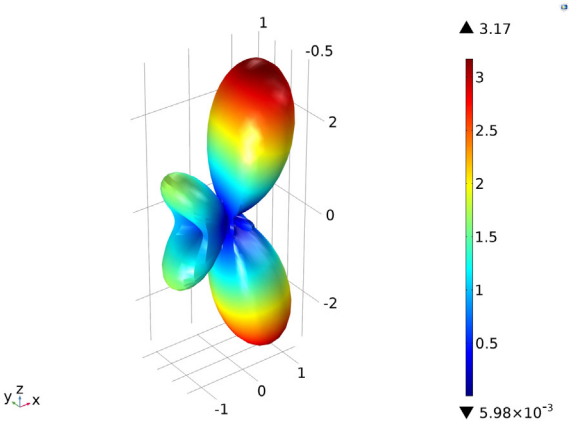

(d) Case 5:Beam steered towards +x direction

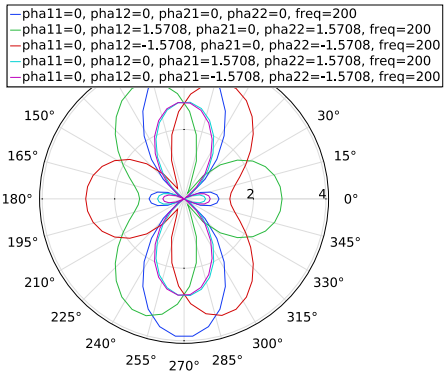

(e) E Far-field pattern as observed in X Plane showing beam steering in Y direction

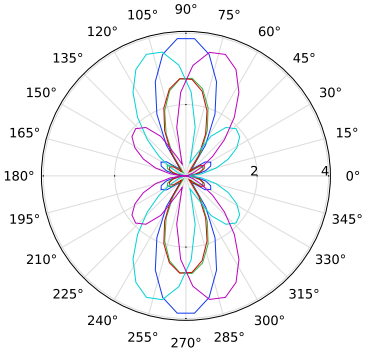

(f) E Far-field pattern as observed in Y Plane showing beam steering in X direction

Fig. 14. The beamsteering performance of the 2X2 antenna array.

Table 2
Phase shift values used for antenna array elements for the beam-steering analysis.

Port name	Phase shift				
	Case 1	Case 2	Case 3	Case 4	Case 5
Antenna 11	0	0	0	0	0
Antenna 12	0	$\pi/2$	$-\pi/2$	0	0
Antenna 21	0	0	0	$\pi/2$	$-\pi/2$
Antenna 22	0	$\pi/2$	$-\pi/2$	$\pi/2$	$-\pi/2$
Beam direction	90 degrees to array	Towards: $-y$ axis	Towards: $+y$ axis	Towards: $-x$ axis	Towards: $+x$ axis

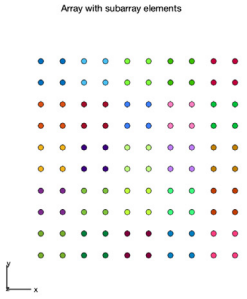

(a) Array arrangement of a slotted beamforming architecture.

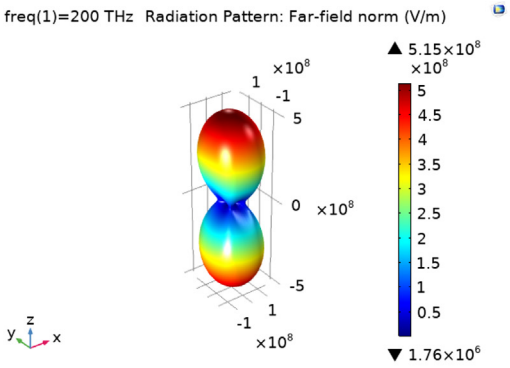

(b) Far field analysis of slotted beamforming architecture.

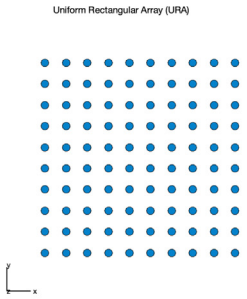

(c) Array arrangement of an adaptive beamforming architecture.

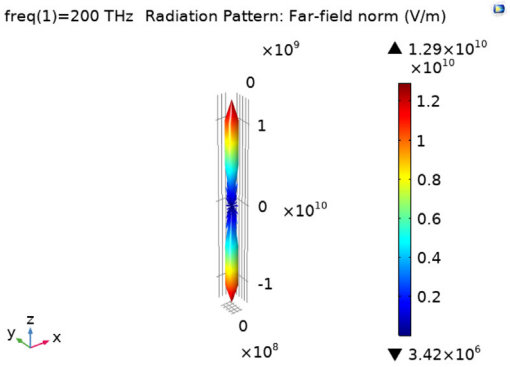

(d) Far field analysis of adaptive beamforming architecture.

Fig. 15. Performance comparison of slotted vs adaptive bow-tie antenna array architectures.

Declaration of competing interest

The authors declare that they have no known competing financial interests or personal relationships that could have appeared to influence the work reported in this paper.

Acknowledgment

This work was supported by the U.S. National Science Foundation (NSF) under Grants No. IIP-1718177, CBET-1706050, and CBET-2039189.

References

[1] J.A. Jackman, A.R. Ferhan, N.-J. Cho, Nanoplasmonic sensors for biointerfacial science, Chem. Soc. Rev. 46 (12) (2017) 3615–3660, http://dx.doi.org/10.1039/C6CS00494F.

[2] H. Im, H. Shao, Y.I. Park, V.M. Peterson, C.M. Castro, R. Weissleder, H. Lee, Label-free detection and molecular profiling of exosomes with a nano-plasmonic sensor, Nature Biotechnol. 32 (5) (2014) 490–495, http://dx.doi.org/10.1038/nbt.2886.

[3] L. Polavarapu, L.M. Liz-Marzán, Towards low-cost flexible substrates for nanoplasmonic sensing, Phys. Chem. Chem. Phys. 15 (15) (2013) 5288–5300, http://dx.doi.org/10.1039/C2CP43642F.

[4] M.I. Stockman, Nanoplasmonic sensing and detection, Science 348 (6232) (2015) 287–288, http://dx.doi.org/10.1126/science.aaa6805.

[5] J.M. Jornet, Y. Bae, C.R. Handelmann, B. Decker, A. Balcerak, A. Sangwan, P. Miao, A. Desai, L. Feng, E.K. Stachowiak, M.K. Stachowiak, Optogenomic interfaces: bridging biological networks with the electronic digital world, Proc. IEEE 107 (7) (2019) 1387–1401, http://dx.doi.org/10.1109/JPROC.2019.2916055.

[6] K. Deisseroth, Optogenetics: 10 years of microbial opsins in neuroscience, Nature Neurosci. 18 (9) (2015) 1213–1225, http://dx.doi.org/10.1038/nn.4091.

[7] S. Busschaert, N. Flöry, S. Papadopoulos, M. Parzefall, S. Heeg, L. Novotny, Beam steering with a nonlinear optical phased array antenna, Nano Lett. 19 (9) (2019) 6097–6103, http://dx.doi.org/10.1021/acs.nanolett.9b02029, http://arxiv.org/abs/1905.09115.

[8] R. Adato, A.A. Yanik, J.J. Amsden, D.L. Kaplan, F.G. Omenetto, M.K. Hong, S. Erramilli, H. Altug, Ultra-sensitive vibrational spectroscopy of protein monolayers with plasmonic nanoantenna arrays, Proc. Natl. Acad. Sci. 106 (46) (2009) 19227–19232, http://dx.doi.org/10.1073/pnas.0907459106.

[9] P. Ghenuche, S. Cherukulappurath, T.H. Taminiau, N.F. van Hulst, R. Quidant, Spectroscopic mode mapping of resonant plasmon nanoantennas, Phys. Rev. Lett. 101 (11) (2008) 116805, http://dx.doi.org/10.1103/PhysRevLett.101.116805.

[10] L. Tang, S.E. Kocabas, S. Latif, A.K. Okyay, D.-S. Ly-Gagnon, K.C. Saraswat, D.A.B. Miller, Nanometre-scale germanium photodetector enhanced by a near-infrared dipole antenna, Nat. Photon. 2 (4) (2008) 226–229, http://dx.doi.org/10.1038/nphoton.2008.30.

[11] L. Novotny, Effective wavelength scaling for optical antennas, Phys. Rev. Lett. 98 (26) (2007) 266802, http://dx.doi.org/10.1103/PhysRevLett.98.266802.

[12] M. Kaniber, K. Schraml, A. Regler, J. Bartl, G. Glashagen, F. Flassig, J. Wierzbowski, J. Finley, Surface plasmon resonance spectroscopy of single bowtie nano-antennas using a differential reflectivity method, Sci. Rep. 6 (1) (2016) 1–10.

[13] C. Moreno, J. Méndez-Lozoya, G. González, F.J. González, G. Boreman, Near-field analysis of discrete bowtie plasmonic nanoantennas, Microw. Opt. Technol. Lett. 62 (2) (2020) 943–948.

[14] N. Zhao, J.-X. Yin, G. Cheng, Y.-M. Wu, W.-D. Hu, X. Lv, Noncoplanar optical bow-tie shaped nanoantenna and array for near-field enhancement, in: 2017 10th UK-Europe-China Workshop on Millimetre Waves and Terahertz Technologies (UCMMT), 2017, pp. 1–3, http://dx.doi.org/10.1109/UCMMT.2017.8068474.

[15] D. Dregely, R. Taubert, J. Dorfmüller, R. Vogelgesang, K. Kern, H. Giessen, 3D optical yagi–uda nanoantenna array, Nature Commun. 2 (1) (2011) 1–7, http://dx.doi.org/10.1038/ncomms1268.
[16] T. Kosako, Y. Kadoya, H.F. Hofmann, Directional control of light by a nano-optical yagi–uda antenna, Nat. Photon. 4 (5) (2010) 312–315, http://dx.doi.org/10.1038/nphoton.2010.34.
[17] O. Caytan, L. Bogaert, G. Torfs, J. Bauwelinck, P. Demeester, D. Vande Ginste, S. Lemey, H. Rogier, Air-filled substrate-integrated-waveguide cavity-backed slot antenna with optical feeding, in: 2nd URSO AT-RASC, 2018, p. 1.
[18] H. Guo, T.P. Meyrath, T. Zentgraf, N. Liu, L. Fu, H. Schweizer, H. Giessen, Optical resonances of bowtie slot antennas and their geometry and material dependence, Opt. Express 16 (11) (2008) 7756–7766, http://dx.doi.org/10.1364/OE.16.007756.
[19] Y. Park, J. Kim, Y.-G. Roh, Q.-H. Park, Optical slot antenna and its application, in: Ultrafast Phenomena and Nanophotonics XXI, Vol. 10102, International Society for Optics and Photonics, 2017, 1010203, http://dx.doi.org/10.1117/12.2250466.
[20] C. Zhao, Y. Liu, J. Yang, J. Zhang, Single-molecule detection and radiation control in solutions at high concentrations via a heterogeneous optical slot antenna, Nanoscale 6 (15) (2014) 9103–9109, http://dx.doi.org/10.1039/C4NR01407C.
[21] R. Esteban, T. Teperik, J.-J. Greffet, Optical patch antennas for single photon emission using surface plasmon resonances, Phys. Rev. Lett. 104 (2) (2010) 026802.
[22] L. Yousefi, A.C. Foster, Waveguide-fed optical hybrid plasmonic patch nano-antenna, Opt. Express 20 (16) (2012) 18326–18335, http://dx.doi.org/10.1364/OE.20.018326.
[23] P. Biagioni, J.S. Huang, L. Duò, M. Finazzi, B. Hecht, Cross resonant optical antenna, Phys. Rev. Lett. 102 (25) (2009) 256801, http://dx.doi.org/10.1103/PhysRevLett.102.256801.
[24] G. Seniutinas, A. Balčytis, I. Reklaitis, F. Chen, J. Davis, C. David, S. Juodkazis, Tipping solutions: emerging 3D nano-fabrication/ -imaging technologies, Nanophotonics 6 (5) (2017) 923–941, http://dx.doi.org/10.1515/nanoph-2017-0008.
[25] B. Zhang, M. Zhang, T. Cui, Low-cost shrink lithography with sub-22nm resolution, Appl. Phys. Lett. 100 (13) (2012) 133113, http://dx.doi.org/10.1063/1.3697836.
[26] L. Zheng, K. Kurselis, A. El-Tamer, U. Hinze, C. Reinhardt, L. Overmeyer, B. Chichkov, Nanofabrication of high-resolution periodic structures with a gap size below 100 nm by two-photon polymerization, Nanoscale Res. Lett. 14 (1) (2019) 134, http://dx.doi.org/10.1186/s11671-019-2955-5.
[27] J. Kern, R. Kullock, J. Prangsma, M. Emmerling, M. Kamp, B. Hecht, Electrically driven optical antennas, Nat. Photon. 9 (9) (2015) 582–586, http://dx.doi.org/10.1038/nphoton.2015.141.
[28] M. Parzefall, L. Novotny, Optical antennas driven by quantum tunneling: A key issues review, Rep. Progr. Phys. 82 (11) (2019) 112401, http://dx.doi.org/10.1088/1361-6633/ab4239.
[29] T. Ali, A.W. Mohammad Saadh, R.C. Biradar, J. Anguera, A. Andújar, A miniaturized metamaterial slot antenna for wireless applications, AEU - Int. J. Electron. Commun. 82 (2017) 368–382, http://dx.doi.org/10.1016/j.aeue.2017.10.005.
[30] J. Liu, Z. Hong, Mechanically tunable dual frequency THz metamaterial filter, Opt. Commun. 426 (2018) 598–601, http://dx.doi.org/10.1016/j.optcom.2018.06.019.
[31] J. Čtyroký, J.G. Wangüemert-Pérez, P. Kwiecien, I. Richter, J. Litvik, J.H. Schmid, Í. Molina-Fernández, A. Ortega-Moñux, M. Dado, P. Cheben, Design of narrowband bragg spectral filters in subwavelength grating metamaterial waveguides, Opt. Express 26 (1) (2018) 179–194, http://dx.doi.org/10.1364/OE.26.000179.
[32] A. Bacigalupo, G. Gnecco, Metamaterial filter design via surrogate optimization, J. Phys. Conf. Ser. 1092 (2018) 012043, http://dx.doi.org/10.1088/1742-6596/1092/1/012043.
[33] Y. Zhao, A. Qing, Y. Meng, Z. Song, C. Lin, Dual-band circular polarizer based on simultaneous anisotropy and chirality in planar metamaterial, Sci. Rep. 8 (1) (2018) 1729, http://dx.doi.org/10.1038/s41598-017-17976-w.
[34] H. Hemmati, H. Hemmati, P. Bootpakdeetam, R. Magnusson, Metamaterial polarizer providing principally unlimited extinction, Opt. Lett. 44 (22) (2019) 5630–5633, http://dx.doi.org/10.1364/OL.44.005630.
[35] N. Yu, F. Capasso, Flat optics with designer metasurfaces, Nature Mater. 13 (22) (2014) 139–150, http://dx.doi.org/10.1038/nmat3839.
[36] R. Renault, N. Sukenik, S. Descroix, L. Malaquin, J.-L. Viovy, J.-M. Peyrin, S. Bottani, P. Monceau, E. Moses, M. Vignes, Combining microfluidics, optogenetics and calcium imaging to study neuronal communication in vitro, PLOS ONE 10 (4) (2015) e0120680, http://dx.doi.org/10.1371/journal.pone.0120680.
[37] F. Schmid, L. Wachsmuth, M. Schwalm, P.-H. Prouvot, E.R. Jubal, C. Fois, G. Pramanik, C. Zimmer, C. Faber, A. Stroh, Assessing sensory versus optogenetic network activation by combining (o)fMRI with optical ca2+ recordings:, J. Cereb. Blood Flow. Metab. (2015) http://dx.doi.org/10.1177/0271678X15619428.
[38] M.K. Stachowiak, E.K. Stachowiak, Evidence-based theory for integrated genome regulation of ontogeny–an unprecedented role of nuclear FGFR1 signaling, J. Cell. Physiol. 231 (6) (2016) 1199–1218, http://dx.doi.org/10.1002/jcp.25298.
[39] R.L. Rich, D.G. Myszka, Advances in surface plasmon resonance biosensor analysis, Curr. Opin. Biotechnol. 11 (1) (2000) 54–61.
[40] X. Zeng, Y. Yang, N. Zhang, D. Ji, X. Gu, J.M. Jornet, Y. Wu, Q. Gan, Plasmonic interferometer array biochip as a new mobile medical device for cancer detection, IEEE J. Sel. Top. Quantum Electron. 25 (1) (2018) 1–7.
[41] S. Gong, X. Lu, D.T. Hoang, D. Niyato, L. Shu, D.I. Kim, Y.-C. Liang, Towards smart wireless communications via intelligent reflecting surfaces: a contemporary survey, IEEE Commun. Surv. Tutor. (2020) 1, http://dx.doi.org/10.1109/COMST.2020.3004197.
[42] M. Najafi, R. Schober, Intelligent reflecting surfaces for free space optical communications, in: 2019 IEEE Global Communications Conference (GLOBECOM), 2019, pp. 1–7, http://dx.doi.org/10.1109/GLOBECOM38437.2019.9013840.
[43] Ö. Özdogan, E. Björnson, E.G. Larsson, Intelligent reflecting surfaces: physics, propagation, and pathloss modeling, IEEE Wirel. Commun. Lett. 9 (5) (2020) 581–585, http://dx.doi.org/10.1109/LWC.2019.2960779.
[44] Q. Wu, R. Zhang, Towards smart and reconfigurable environment: intelligent reflecting surface aided wireless network, IEEE Commun. Mag. 58 (1) (2020) 106–112, http://dx.doi.org/10.1109/MCOM.001.1900107.
[45] X. Hao, C. Kuang, Z. Gu, Y. Wang, S. Li, Y. Ku, Y. Li, J. Ge, X. Liu, From microscopy to nanoscopy via visible light, Light Sci. Appl. 2 (10) (2013) e108, http://dx.doi.org/10.1038/lsa.2013.64.
[46] M.J. Horton, O.S. Ojambati, R. Chikkaraddy, W.M. Deacon, N. Kongsuwan, A. Demetriadou, O. Hess, J.J. Baumberg, Nanoscopy through a plasmonic nanolens, Proc. Natl. Acad. Sci. 117 (5) (2020) 2275–2281, http://dx.doi.org/10.1073/pnas.1914713117.
[47] E. Wertz, B.P. Isaacoff, J.D. Flynn, J.S. Biteen, Single-molecule super-resolution microscopy reveals how light couples to a plasmonic nanoantenna on the nanometer scale, Nano Lett. 15 (4) (2015) 2662–2670, http://dx.doi.org/10.1021/acs.nanolett.5b00319.
[48] J. Dorfmuller, R. Vogelgesang, W. Khunsin, C. Rockstuhl, C. Etrich, K. Kern, Plasmonic nanowire antennas: experiment, simulation, and theory, Nano Lett. 10 (9) (2010) 3596–3603.
[49] H. Raether, Surface plasmons on gratings, in: Surface Plasmons on Smooth and Rough Surfaces and on Gratings, Springer, 1988, pp. 91–116.
[50] L. Novotny, B. Hecht, Principles of Nano-Optics, Cambridge university press, 2012.
[51] G. Stegeman, J. Burke, D. Hall, Nonlinear optics of long range surface plasmons, Appl. Phys. Lett. 41 (10) (1982) 906–908.
[52] C.A. Balanis, Antenna theory: A review, Proc. IEEE 80 (1) (1992) 7–23.
[53] M. Nafari, J.M. Jornet, Metallic plasmonic nano-antenna for wireless optical communication in intra-body nanonetworks, in: Proceedings of the 10th EAI International Conference on Body Area Networks, ICST (Institute for Computer Sciences, Social-Informatics and Telecommunications Engineering), 2015, pp. 287–293.
[54] M. Nafari, J.M. Jornet, Modeling and performance analysis of metallic plasmonic nano-antennas for wireless optical communication in nanonetworks, IEEE Access 5 (2017) 6389–6398.
[55] L. Zakrajsek, E. Einarsson, N. Thawdar, M. Medley, J.M. Jornet, Design of graphene-based plasmonic nano-antenna arrays in the presence of mutual coupling, in: Antennas and Propagation (EuCAP), 2017 11th European Conference on, IEEE, 2017, pp. 1381–1385.
[56] C. Han, J.M. Jornet, I. Akyildiz, Ultra-massive MIMO channel modeling for graphene-enabled terahertz-band communications, in: 2018 IEEE 87th Vehicular Technology Conference (VTC Spring), IEEE, 2018, pp. 1–5.
[57] C.A. Balanis, P.I. Ioannides, Introduction to smart antennas, Synth. Lect. Antennas 2 (1) (2007) 1–175.
[58] A. Melikyan, L. Alloatti, A. Muslija, D. Hillerkuss, P. Schindler, J. Li, R. Palmer, D. Korn, S. Muehlbrandt, D. Van Thourhout, et al., High-speed plasmonic phase modulators, Nat. Photon. 8 (3) (2014) 229.
[59] C. Haffner, D. Chelladurai, Y. Fedoryshyn, A. Josten, B. Baeuerle, W. Heni, T. Watanabe, T. Cui, B. Cheng, S. Saha, et al., Low-loss plasmon-assisted electro-optic modulator, Nature 556 (7702) (2018) 483–486.
[60] W. Heni, Y. Fedoryshyn, B. Baeuerle, A. Josten, C.B. Hoessbacher, A. Messner, C. Haffner, T. Watanabe, Y. Salamin, U. Koch, et al., Plasmonic IQ modulators with attojoule per bit electrical energy consumption, Nat. Commun. 10 (1) (2019) 1–8.

[61] C. Haffner, W. Heni, Y. Fedoryshyn, J. Niegemann, A. Melikyan, D.L. Elder, B. Baeuerle, Y. Salamin, A. Josten, U. Koch, et al., All-plasmonic Mach–Zehnder modulator enabling optical high-speed communication at the microscale, Nat. Photon. 9 (8) (2015) 525–528.

[62] P. Laferrière, E. Yeung, L. Giner, S. Haffouz, J. Lapointe, G.C. Aers, P.J. Poole, R.L. Williams, D. Dalacu, Multiplexed single-photon source based on multiple quantum dots embedded within a single nanowire, Nano Lett. 20 (5) (2020) 3688–3693, http://dx.doi.org/10.1021/acs.nanolett.0c00607.

[63] P. Miao, Z. Zhang, J. Sun, W. Walasik, S. Longhi, N.M. Litchinitser, L. Feng, Orbital angular momentum microlaser, Science 353 (6298) (2016) 464–467.

Amit Sangwan received his Bachelor of Technology in Electronics and Communication Engineering degree from Guru Jambheshwar University of Science and Technology, Hisar, Haryana, India in 2013. He received his Master of Science degree in Electrical Engineering from University at Buffalo, The State University of New York, Buffalo, NY, USA, in 2017 and is currently pursuing his Ph.D. degree at Department of Electrical and Computer Engineering at Northeastern University, Boston, USA under the guidance of Dr. Josep M. Jornet. He worked as the Research and Development Engineer at Technology Uncorked an innovative start-up company, India from August 2013 to June 2015. He completed a summer internship in 2018 at MERL (Mitsubishi Electric Research Labs), Boston, MA on advanced antenna array design. His current research interests are in the field of IoT (internet of things), nano-sensor networks, nano-optical antennas, antenna design and beamforming, Ultra-broadband communications, wireless optical communication, and bio-nano implant communications.

Josep Miquel Jornet is an Associate Professor in the Department of Electrical and Computer Engineering, the Director of the Ultrabroadband Nanonetworking Laboratory and a Member of the Institute for the Wireless Internet of Things as well as the SMART Center at Northeastern University, in Boston, MA, since 2019. He received the B.S. in Telecommunication Engineering and the M.Sc. in Information and Communication Technologies from the Universitat Politecnica de Catalunya, Barcelona, Spain, in 2008. He received the Ph.D. degree in Electrical and Computer Engineering from the Georgia Institute of Technology (Georgia Tech), Atlanta, GA, in 2013. From September 2007 to December 2008, he was a visiting researcher at the Massachusetts Institute of Technology (MIT), Cambridge, under the MIT Sea Grant program. Between August 2013 and August 2019, he was a faculty with the Department of Electrical Engineering at the University at Buffalo, The State University of New York. His research interests are in terahertz communication networks, wireless nano-bio-communication networks, and the Internet of Nano-Things. In these areas, he has co-authored more than 160 peer-reviewed scientific publications, one book, and has also been granted 4 US patents. Since July 2016, he is the Editor-in-Chief of the Nano Communication Networks (Elsevier) Journal. He is serving as the lead PI on multiple grants from U.S. federal agencies, including the National Science Foundation, the Air Force Office of Scientific Research, and the Air Force Research Laboratory. He is a recipient of the National Science Foundation CAREER award and several other awards from IEEE, ACM, UB, and Northeastern University.